ELSEVIER

Contents lists available at ScienceDirect

Aquatic Toxicology

journal homepage: www.elsevier.com/locate/aqtox



How relevant are sterols in the mode of action of prymnesins?

Hélène-Christine Prause ^{a,b}, Deniz Berk ^a, Catharina Alves-de-Souza ^{c,d}, Per J. Hansen ^e, Thomas O. Larsen ^f, Doris Marko ^a, Giorgia Del Favero ^{a,g}, Allen Place ^h, Elisabeth Varga ^{a,i,*}

- a Department of Food Chemistry and Toxicology, Faculty of Chemistry, University of Vienna, Währinger Str. 38-40, 1090 Vienna, Austria
- ^b Vienna Doctoral School in Chemistry, Faculty of Chemistry, University of Vienna, Währinger Str. 42, 1090 Vienna Austria
- c Departamento de Oceanografía, Facultad de Ciencias Naturales y Oceanográficas, Universidad de Concepción, Concepción 4030000, Chile
- ^d Centro de Investigación Oceanográfica COPAS Coastal, Universidad de Concepción, Concepción, Chile
- ^e Marine Biological Section, Department of Biology, University of Copenhagen, Strandpromenaden 5, 3000 Elsinore, Denmark
- f Department of Biotechnology and Biomedicine, Technical University of Denmark, Søltofts Plads 221, 2800 Kgs. Lyngby, Denmark
- g Core Facility Multimodal Imaging, Faculty of Chemistry, University of Vienna, Währinger Str. 38-42, 1090 Vienna, Austria
- h Institute of Marine and Environmental Technology, University of Maryland Center for Environmental Science, 701 E. Pratt Street, Baltimore, MD 21202, USA
- ⁱ Unit Food Hygiene and Technology, Centre for Food Science and Veterinary Public Health, Clinical Department for Farm Animals and Food System Science, University of Veterinary Medicine, Vienna, Veterinärplatz 1, 1210 Vienna, Austria

ARTICLE INFO

Keywords: Prymnesium parvum Cholesterol RTgill-W1 Toxin mixture Hemolysis Cytotoxicity

ABSTRACT

Prymnesins, produced by the haptophyte Prymnesium parvum, are considered responsible for fish kills when this species blooms, Although their toxic mechanism is not fully understood, membrane disruptive properties have been ascribed to A-type prymnesins. Currently it is suggested that pore-formation is the underlying cause of cell disruption. Here the hypothesis that A-, B-, and C-type prymnesins interact with sterols in order to create pores was tested. Prymnesin mixtures containing various analogs of the same type were applied in hemolysis and cytotoxicity assays using Atlantic salmon Salmo salar erythrocytes or rainbow trout RTgill-W1 cells. The hemolytic potency of the prymnesin types reflected their cytotoxic potential, with approximate concentrations reaching 50 % hemolysis (HC50) of 4 nM (A-type), 54 nM (C-type), and 600 nM (B-type). Variabilities in prymnesin profiles were shown to influence potency. Prymnesin-A (3 Cl) + 2 pentose + hexose was likely responsible for the strong toxicity of A-type samples. Co-incubation with cholesterol and epi-cholesterol prehemolysis reduced the potential by about 50 % irrespective of sterol concentration, suggesting interactions with sterols. However, this effect was not observed in RTgill-W1 toxicity. Treatment of RTgill-W1 cells with 10 µM lovastatin or 10 μM methyl- β -cyclodextrin-cholesterol modified cholesterol levels by 20-30 %. Regardless, prymnesin cytotoxicity remained unaltered in the modified cells. SPR data showed that B-type prymnesins likely bound with a single exponential decay while A-types seemed to have a more complex binding. Overall, interaction with cholesterol appeared to play only a partial role in the cytotoxic mechanism of pore-formation. It is suggested that prymnesins initially interact with cholesterol and stabilize pores through a subsequent, still unknown mechanism possibly including other membrane lipids or proteins.

1. Introduction

The haptophyte *Prymnesium parvum* is considered one of the most persistent harmful algal bloom-forming microalgae in brackish water (Hallegraeff, 1993; Kaartvedt *et al.*, 1991). It was recently (2022) the cause of a massive bloom followed by a major fish-killing event in the Oder/Odra River in Europe (Free *et al.*, 2023). *P. parvum* produces a group of toxins called prymnesins which have ichthyotoxic and hemolytic effects and are believed to be the cause of fish kills ensuing from

such blooms (Binzer et al., 2019; Igarashi et al., 1999, Igarashi et al., 1996; Rasmussen et al., 2016; Yariv and Hestrin, 1961). Currently, prymnesins are characterized as either A-, B-, and C-types, depending on the length of their carbon-backbone (Binzer et al., 2019; Rasmussen et al., 2016). To date, only four structures have been fully elucidated (Igarashi et al., 1996; Igarashi et al., 1999; Rasmussen et al., 2016). Many different analogs have been found since, for which no elucidation has been performed, with varying degrees of chlorination and glycosylation. The structure of C-type prymnesins remains to be elucidated. It was

E-mail address: Elisabeth.Varga@vetmeduni.ac.at (E. Varga).

^{*} Corresponding author.

suggested that prymnesin toxicity is pH-dependent, which has been tentatively examined previously (Caron et al., 2023; Igarashi et al., 1998; Moran & Ilani, 1974; Shilo and Aschner, 1953; Ulitzur and Shilo, 1964). A common feature all identified prymnesins share is a primary amine in their lipophilic moiety (Igarashi et al., 1999, Igarashi et al., 1996; Rasmussen et al., 2016). The protonation of this amine group is believed to play an important role in the "charge distribution" of the molecule and thus its toxicity (Igarashi et al., 1998; Moran & Ilani, 1974; Valenti et al., 2010). While changes in pH may modify toxin activity, the hypothesis of reduced toxicity at pH 6.5 due to larger relative amounts of ionized prymnesins as suggested by Valenti et al., (2010) is debated and further research is needed to elucidate the relationship between prymnesin toxicity and pH (Cichewicz and Hambright 2010). Differences in the potential of the three groups have been shown for ichthyotoxic as well as cytotoxic potential (Blossom et al., 2014; Rasmussen et al., 2016; Varga and Prause et al., 2024). Interestingly, one strain of P. parvum can only produce one type of toxin, namely A, B, or C, but various analogs thereof (Binzer et al., 2019; Rasmussen et al., 2016).

Upon contact with the fish gills, prymnesins can increase cell membrane permeability, wreaking havoc on the osmotic balance, ultimately causing the fish to succumb to suffocation (Bergsson et al., 2019; Ulitzur and Shilo, 1966; Yariv and Hestrin, 1961). At the molecular level, this effect is supposedly achieved through pore formation in the gill cells (Ulitzur and Shilo, 1966; Yariv and Hestrin, 1961). Despite numerous studies and the current knowledge on prymnesins at the time of writing, it remains unclear how prymnesins can accomplish such damage to the fish gill cells. Given their structural similarities to karlotoxin, with a terminally chlorinated aliphatic chain, or to amphidinol, an aliphatic chain without chlorination (Fig. 1), and the currently available toxicity data, it is postulated that prymnesins can interact directly with the cell membrane (Igarashi et al., 1998; Imai and Inoue, 1974; Shilo, 1981; Waters et al., 2015).

This study aimed at providing more detail regarding the mode of action of prymnesins by trying to understand the relevance of sterols in their toxicity. It was hypothesized that prymnesins can interact with cell membrane lipids, such as cholesterol, to exert their toxic effects upon the cells. As the difference in cytotoxicity between the groups has been established already, it was intriguing whether this would be the case for their hemolytic potency as well. To answer the question of whether prymnesins are able to interact with sterols, hemolysis as well as

cytotoxicity were tested for toxins that had previously been combined with sterols. In addition, RTgill-W1 cell membranes were modified to either contain more or less cholesterol and subsequently exposed to prymnesins. This would help better understand the relevance of membrane cholesterol for the cytotoxic mechanism of prymnesins, and whether the exertion of toxic activity is dependent on the levels of cholesterol in the membrane. Moreover, it was of interest to examine if variances in analog profiles would influence the toxicity. Two A-type and two B-type strains were used for this comparison. Finally, the interactions between A- and B-type prymnesins with selected sterols were also recorded via surface plasmon resonance (SPR) measurements.

2. Materials and methods

2.1. Samples

Prymnesin samples were obtained from biomass of *P. parvum* cultures. One A-type prymnesin sample, originally a hemolysis solution from Sigma Aldrich (No. P-1389, St. Louis, MO, USA), was kindly gifted by T. Shier (Department of Medicinal Chemistry, College of Pharmacy, University of Minnesota, MN, USA). Another A-type and one B-type strain were cultivated and harvested by the Algal Resources Collection (ARC) in the Center of Marine Sciences at the Marine Biotechnology in North Carolina, University of North Carolina at Wilmington (strains UNCW-ARC140 and UNCW-ARC66, respectively). One B-type strain (K-0081), was obtained from the Scandinavian Culture Collection of Algae and Protozoa (SCCAP, now incorporated in the Norwegian Culture Collection of Algae, NORCCA). Lastly, the C-type strain RCC-1436 was purchased from the Roscoff Culture Collection (RCC, France).

Culture conditions for *P. parvum* strains were previously described in Varga and Prause *et al.* (2024) and briefly described as follows. For strains UNCW-ARC140 and UNCW-ARC66, F/2 medium was prepared from filtered and autoclaved natural seawater collected 40 miles off the Wilmington coast and adjusted to 4 ppt. The microalgae were cultivated with an initial density of \sim 1,000 cells mL⁻¹ in a 10-L photobioreactor (IKA Algaemaster 10 control, IKA® Works Inc., Wilmington, NC, USA) at 20 °C, 70 μ mol m⁻² s⁻¹ and a 12:12 dark:light photoperiod (LED Light). Air bubbling and CO₂ injection were used to maintain a pH \sim 8. Cells counts were determined every 3 days using a Sedwick-Rafter chamber and cells were harvested after 2 weeks (190,000 cells mL⁻¹) by

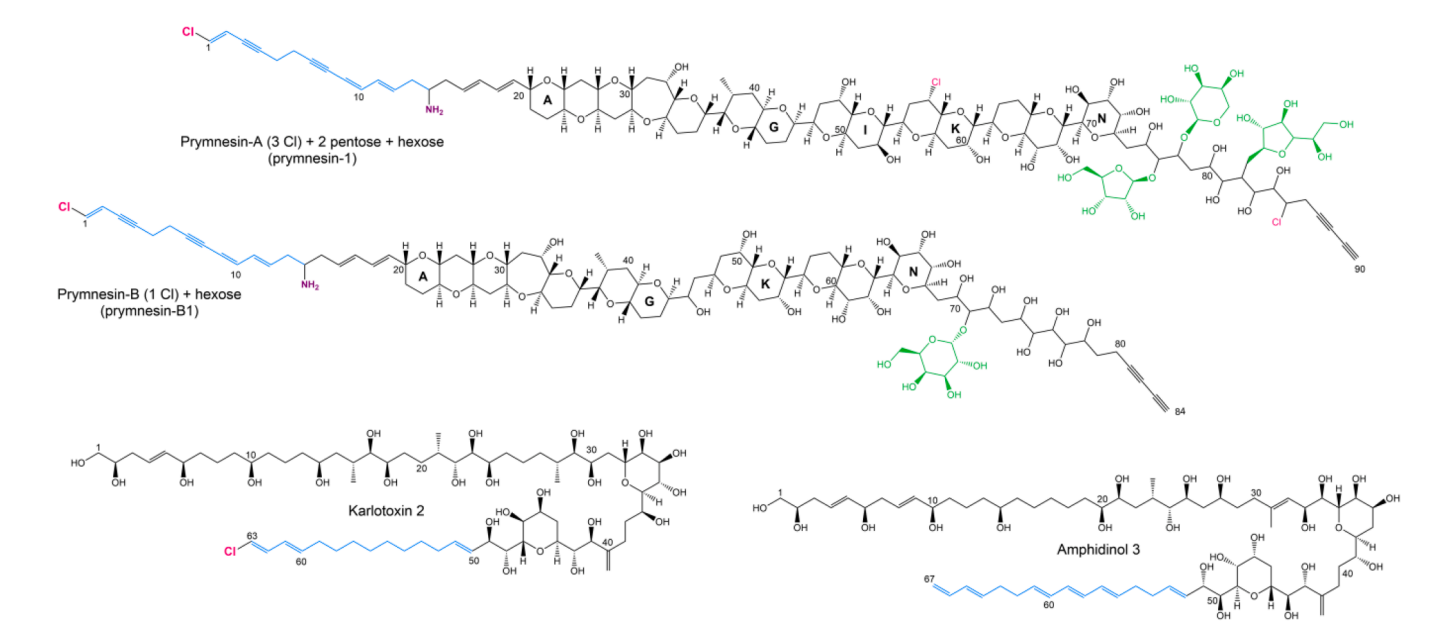


Fig. 1. Structures of one A- type and one B-type prymnesin, respectively, from the haptophyte Prymnesium parvum as examples for comparison to dinoflagellate toxins karlotoxin 2 from Karlodinium veneficum and amphidinol 3 from Amphidinium klebsii.

centrifugation in a Sorvall superspeed RC2-B centrifuge at 4 $^{\circ}C$ and 12, 000 \times g. For strains K-0081 and RCC-1436. For strains K-0668 and RCC-1436 F/2 medium was prepared from filtered and pasteurized natural seawater off the coast of Elsinore at 30 ppt (Guillard, 1975). The microalgae were maintained in 10-L glass bottles, at 15 $^{\circ}C$ with a 14:10 h light-dark cycle and 450-500 μmol photons m^{-2} s $^{-1}$ irradiance. Cell concentrations were monitored every two to three days by manual cell counting under the microscope to ensure these strains remained in the exponential growth phase. The algal biomass of all strains was harvested in the late exponential phase by centrifugation at 4,000 relative centrifugal force (rcf) for 15 min at 4 $^{\circ}C$, and the biomass pellet separated from the supernatant.

For all the strains, the pellets were then stored at -80 °C until extraction using the protocol provided by Binzer et al. (2019). First, the algal cell pellet was thawed, then centrifuged at 4,000 rcf for 5 min to remove any remaining supernatant. Second, the pellets were extracted several times with ice-cold acetone to remove chlorophyll, until a light green supernatant was obtained. Third, prymnesins were subsequently extracted with methanol (MeOH). The MeOH was then evaporated with a rotavapor (R-114, Büchi Labortechnik AG, Flawil, Switzerland) or a CentriVap Benchtop Vacuum Concentrator coupled to a CentriVap Coldtrap (both Labconco Corp., Kansas City, MO, USA), and the samples were reconstituted in absolute ethanol (EtOH). Finally, the samples were placed in an ultrasonic bath for several minutes, centrifuged, and the particle-free supernatant was transferred to HPLC vials and stored at -20 °C. The two A-type samples will henceforward be referred to as the A-type solution (Sigma Aldrich) and the A-type extract, from Sigma Aldrich of unknown strain origin and strain UNCW-ARC140 respectively.

2.1.1. Prymnesin profiles

The prymnesin profile was analyzed using ultra-high performance liquid chromatography coupled with high-resolution mass spectrometry (UHPLC-HRMS) exactly as described in Varga and Prause et al. (2024). Toxin concentrations for prymnesin samples were estimated through high-performance liquid chromatography and fluorescence detection (HPLC-FLD), as previously described (Svenssen et al., 2019; Varga and Prause et al., 2024). In short, prymnesins were labeled with a fluorescent tag (AccQ-Tag Fluor Reagent Kit, Waters Corp., Milford, MA, USA) through derivatization of their primary amines. A 1200 HPLC system (Agilent Technologies, Waldbronn, DE), using an Agilent Poroshell C18 column (2.1 \times 50 mm 2.7 μ m) with water as eluent A and acetonitrile as eluent B, both containing 0.1 % formic acid, were used for chromatographic separation. Prymnesins were detected via fluorescence at excitation/emission wavelengths of 250/395 nm. The data were analyzed with ChemStation for LC Rev. B.04.01 SP1 from Agilent Technologies.

2.2. Cell culture

Both the rainbow trout (*Oncorynchus mykiss*) gill cell line RTgill-W1, obtained from K. Schirmer (Department of Environmental Toxicology, EAWAG, Dübendorf, CH), and the human epithelial colon cell line HCEC-1CT, provided by J. W. Shay, UT Southwestern Medical Center, Dallas, TX, USA, were chosen for cytotoxicity tests and cultivated as described in Varga and Prause *et al.*, (2024).

RTgill-W1 cells were kept at 19 °C in Leibovitz's 15 medium (L-15) supplemented with 1 % (ν/ν) penicillin/streptomycin (Thermo Fisher Scientific, Waltham, MA, USA) and 10 % (ν/ν) fetal calf serum (EuroBio, Le Ulis, France) (Bols et al., 1994). HCEC-1CT cells were cultured at 37 °C with 5 % CO2 in Dulbecco's Modified Eagle's Medium (DMEM (Thermo Fisher Scientific, Waltham, MA, USA)). For the complete cultivation medium 500 mL DMEM were supplemented with 10 mL Medium 199 (10x), 10 mL HEPES buffer solution 1 M, 5.2 mL Insulin-Transferrin-Selenium-G Supplement (Thermo Fisher Scientific, Waltham, MA, USA), 10 mL HyCloneTM Cosmic CalfTM Serum (GE Healthcare Life Sciences HyClone Laboratories, Danaher Corp.,

Washington DC, USA), 0.6 mL gentamycin solution (Sigma Aldrich GmbH, St. Louis, MO, USA), 100 μ L Recombinant Human Epidermal Growth Factor (100 μ g/mL, Szabo-Scandic HandelsgmbH & Co KG, Vienna, Austria), and 100 μ L hydrocortisone (5 mg/mL, Merck KGaA, Darmstadt, Germany). Both cell lines were kept in cell+ surface (Sarstedt AG & Co KG, Nürnbrecht, Germany) flasks or plates.

2.3. Toxicity tests

2.3.1. Cell viability assays

Cell viability of RTgill-W1 and HCEC-1CT cells upon exposure to ichthyotoxin samples was mainly determined with the CellTiter-Blue® (CTB (Promega, Madison, WI, USA)) assay according to the manufacturer's instructions. The protocol used for exposing RTgill-W1 cells to ichthyotoxins was adapted from the one described previously (Dayeh et al., 2005; Rasmussen et al. 2016) Cells were seeded onto an F-bottom 96-well polystyrene plate at a density of 2×10^4 cells per well (RTgill-W1) or 5 \times 10 3 cells per well (HCEC-1CT) and grown for 48 h. Cells were then exposed to $100 \, \mu L$ prymnesin sample diluted in culture medium with a final EtOH concentration of 0.5 % (ν/ν). Medium containing 0.5 % (ν/ν) EtOH was used as solvent control, and medium containing 0.05 % and 0.1 % (v/v) TritonTM X-100 (Sigma Aldrich, St. Louis, MO, USA) as positive control. Following a 3-h incubation at 21 °C (RTgill-W1) or 37 $^{\circ}$ C (HCEC-1CT) in the dark, 100 μ L of 1:10 diluted CTB reagent in culture medium was added to the previously aspirated cells and incubated for 1 h at room temperature in the dark.

The WST-1 Assay (Abcam, Cambridge, United Kingdom) was performed according to the manufacturer's protocol to detect cytotoxicity in RTgill-W1 cells after treatment with cholesterol altering substances (section 2.4.2). After the wells had been aspirated and rinsed with Dulbecco's phosphate buffered saline (DPBS, Thermo Scientific Waltham, MA, USA), 80 μL of WST-1 reagent were added to the wells and incubated for 1.5 h in the dark, after which the absorbance was taken at 450 and 650 nm. The cells were then fixed and stained with a fluorescent dye, visualizing cellular cholesterol (2.4.3).

The lactate dehydrogenase (LDH) assay (Pierce CyQuant TM , Thermo Scientific, Waltham, MA, USA) was used to evaluate lytic effects on the cells. The manufacturer's protocol was followed for LDH testing, where 50 μ L of supernatant were combined with 50 μ L reaction mix. The reaction was stopped after 30 min by adding 50 μ L stop solution, and finally the absorbance was measured at 490 and 680 nm.

2.3.2. Hemolytic assay

Red blood cells (RBCs) from the Atlantic salmon (Salmo salar) were utilized to assess the hemolytic potential of the prymnesin samples with the exception of the extract of strain UNCW-ARC66. The assay protocol was adapted from the one described by Deeds et al. (2002). Blood was drawn from the caudal vein using heparin-treated needles and collected in a falcon tube for centrifuging at 1,250 rcf and 4 °C for 25 min to remove serum. The remaining RBCs were subsequently washed three times (1,250 rcf, 4 °C, 5 min) with cold Tris-buffer I, which consisted of 150 mM NaCl, 3.2 mM KCl, 1.25 mM MgSO₄, 12.2 mM Tris base in MilliQ water. RBCs were then diluted in Tris-buffer II (Tris-buffer I +3.75 mM CaCl₂) to 1.25 % (ν/ν) of their original concentration and stored at 4 °C for up to 10 days. Both buffers were adjusted to pH 7.4 at 10 °C before filter sterilization (0.22 µm). A calibration curve was obtained by preparing a dilution series of the hemolytic reference compound saponin (Quillaja bark, CAS No.: 8047-15-2; Sigma Chemical Co., St. Louis, MO, USA) (Lorent et al., 2014). Hemolytic assays were performed in 96-well plates (V-bottom, polystyrene, non-treated, Corning Inc., Corning, NY, USA) by preparing desired dilutions of the ichthyotoxin samples in Tris-buffer II, with a final EtOH concentration of $0.5\,\%$ (ν/ν) and adding 100 µL sample per well. Hemolysis was started once $100 \,\mu\text{L}$ of 1.25 %-RBC solution were added to the samples. The plate was placed on an orbital shaker (80-100 rotations per minute) and incubated at room temperature for 1 h. The solvent control was 0.5 % EtOH (ν/ν) in

Tris-buffer II, and 8 µg/mL saponin in Tris-buffer II served as positive control. After incubation, the plate was centrifuged at 600 rcf for 5 min, after which 100 µL of the supernatant were transferred into a clear F-bottom 96-well polystyrene plate (Corning Inc., Corning, NY, USA). The absorbance of hemoglobin released from the RBCs was then read at 540 nm. The RBC solution was monitored for its stability by checking the optical density of the solution supernatant without addition of any hemolysins. Ideally the absorbance of the supernatant would remain around 0.2, and the maximal acceptable value was set at 0.4. When an absorbance of $\geq\!0.4$ was reached the solution was discarded and a new batch of 1.25 %-RBC solution was prepared. Sensitivities of the individual batches were tested by obtaining a saponin curve.

The B-type prymnesin extract of strain UNCW-ARC66 was the only sample not tested for hemolysis since it was not able to cause cell viability of RTgill-W1 cells to fall below 50 %, and therefore considered not potent enough.

All experiments involving fish were carried out in accordance with the guidelines at the Institutional Animal Care and Use Committee (IACUC) of the University of Maryland Medical School: protocol No. 0014 and No. 0522012. Fish used for tissue sampling were anesthetized with tricaine methanesulfonate (MS-222, 10 mg/L) for blood sampling and then euthanized with MS-222 (150 mg/L).

2.4. Impact of sterols on toxicity

2.4.1. Combination assays

Possible interactions between prymnesins and cholesterol (5(6)-cholesten-3-ol, Sigma, St. Louis, MO, USA) and epicholesterol (5-cholesten-3a-ol, Steraloids Inc., Newport, RI, USA) were tested in hemolytic assays. Again, the protocol described by Deeds *et al.* (2002) was followed. Briefly, samples (extracts of UNCW-ARC140, K-0081, and RCC-1436, and the Sigma Aldrich prymnesin solution) were diluted to their EC $_{50}$ values and then combined with the equivalent volume of sterol in solution at 0.1-10,000 nM before starting hemolysis assays.

This assay was adapted for cytotoxicity in RTgill-W1 and HCEC-1CT cells. Sterol concentrations were adjusted to range from 1 nM to 50,000 nM for RTgill-W1 and HCEC-1CT cells, in the respective cultivation media. Cells were seeded as per usual, and the A-type prymnesin solution was diluted to twice the concentration of the EC $_{50}$ obtained for either cell line. The sample was then combined with the equivalent volume of sterol at various concentrations, and a total volume of 100 μL was added to the cells, which were then incubated for 3 h. Cell viability was measured in CTB and LDH assays.

Sterols were dissolved in EtOH.

2.4.2. Cholesterol modulation in RTgill-W1 cells

Whether the cytotoxicity of prymnesins is dependent on the cholesterol content of the target cell membrane was assessed via fluorescence microscopy combined with cell viability testing as previously described (Rebhahn et al., 2022). Conditions to achieve a desirable change in membrane cholesterol content while maintaining acceptable cell viability of RTgill-W1 cells were determined as follows: cells were seeded into 96-well plates at a density of 1.5×10^4 cells per well for 48 h followed by a 24 h incubation with the cholesterol content-altering agents. To increase the cholesterol content cells were treated with water-soluble cholesterol in the form of cholesterol-loaded methyl-beta-cyclodextrin (MbCD-Chol, Sigma Aldrich GmbH, St. Louis, MO, USA) at 10 and 50 µM (Del Favero et al., 2020). Lovastatin (lovastatin sodium salt, Enzo, Farmingdale, NY, USA) at 0.1, 1, and 10 µM was used to test for depletion of membrane cholesterol. These treatments were controlled for cytotoxicity in a WST-1 assay while establishing this protocol. Cholesterol was relatively quantified using a fluorescent stain as described in 2.4.3. Based on the results of these testing conditions, MbCD-Chol and lovastatin at 10 μM were chosen for further testing with prymnesins. After the 24-h cholesterol-altering treatment, 100 μL of the A-type prymnesin solution at approximately EC90 (12 nM) and the

UNCW-ARC66 extract (B-type) at approximately EC₆₀ (113 nM) were added to the cells and incubated for 3 h. The resulting cell viability was measured via the CTB assay using the usual controls. As lovastatin was dissolved in dimethylsulfoxide (DMSO), the solvent control for this compound consisted of 0.25 % (ν/ν) DMSO in culture medium.

2.4.3. Fluorescence microscopy

After manipulating the cholesterol content of the cells and cell viability testing through WST-1, the cells were fixed with 1 % (v/v)paraformaldehyde (PFA) in DPBS for 30 min, followed by quenching the PFA with 100 mM glycine in DPBS for 1-2 min. Next, the cholesterol in the cells was stained with filipin III ready-made solution (25 $\mu g/mL$ in DPBS (Sigma Aldrich GmbH, St. Louis, MO, USA) for 1 h. In between all steps and after staining, the cells were rinsed three times with DPBS, and finally ROTI®Mount FluoroCare mounting medium (Carl Roth GmbH + Co. KG, Karlsruhe, Germany) was added to each well. Fluorescence spectra were recorded between excitation at 340-380 nm and emission at 385-470 nm with the Lionheart FX automated microscope (BioTek Instruments Inc., Winooski, VT, USA) using the DAPI channel. For quantification the ImageJ 1.54f Fiji Software was used, where gray-scale images were converted to RBG images, and keeping only the bluechannel image, 7 single cells per image were selected and measured for their area and integrated intensity of filipin fluorescence. The background intensity was measured and subtracted from the intensities obtained for the cells.

2.5. Surface plasmon resonance (SPR)

After performing co-incubation assays of these ichthyotoxins with selected sterols, surface plasmon resonance (SPR) measurements were performed for assessing interactions between the A-type prymnesin solution and the K-0081 extract (B-type) with cholesterol, epicholesterol, and ergosterol (Fluka Chemie GmbH, Buchs, Switzerland). The experiments were run on a T200 Biacore system using the Series S Sensor Chip HPA (Cytiva, Danaher Corp., Washington DC, USA). The three sterols were diluted in HBS buffer (10 mM HEPES, 150 mM NaCl, pH 7.4) to reach a concentration of 10 µM. The sensor chip was prepared by first pre-conditioning all four flow cells (Fc) with 40 mM octyl-D-glucoside for 5 min at a flow rate of 10 µL/min. The sterol were subsequently immobilized at about 1,000 responsive units (RU) with a flowrate of 2 μL/min for 30 min. Fc1 with only octyl-D-glucoside served as control. The baseline was stabilized by rinsing all Fcs with 10 mM NaOH for 30 s, followed by a 5 min blocking with bovine serum albumin (0.1 mg/mL in dH₂O). HBS buffer was run over all Fcs three times, followed by 1 μM of A-type prymnesins (Sigma Aldrich) and 1 μM B-type prymnesin extract (strain K-0081) for 2 min at 10 µL/min. In-between samples the Fcs were washed with HBS buffer. Responses were fitted on a 1:1 model, and kinetic values were calculated with the program Biacore T200 software 3.2.1 (Cytiva, Danaher Corp., Washington DC, USA). As these samples were mixtures of different analogs, SPR served only as a way of confirming whether sterol-interactions take place. Specific reaction kinetics were not calculated, but the overall ability of prymnesins to bind with sterols was tested and compared between the two prymnesin types.

2.6. Statistics

All assays were carried out in technical triplicates, with the exception of SPR assays, which were performed in duplicates. Statistical significance was calculated with One Way ANOVA followed by the posthoc Fisher's least significant difference test, as well as t-test (one-sample or two-sample) using OriginPro 2020 Version 9.7.0.185 (Academic, OriginLab Corporation, Northampton, MA, USA).

3. Results

3.1. Prymnesin profile

The different prymnesin analogs of all the samples were analyzed and are listed in Table 1. Three of the samples had already been reported by Varga and Prause et al. (2024) and are indicated as such. The profiles found for the two A-type samples exhibited various differences. The main components of these samples were analog prymnesin-A (3 Cl) + 2 pentose + hexose (prymnesin-1), making up 60 % of the total prymnesins in the A-type solution (Sigma Aldrich), and analog prymnesin-A (3 Cl) + pentose (prymnesin-2), with 43 % in the extract UNCW-ARC140. Only about 20 % of analog prymnesin-A (3 Cl) + 2 pentose + hexose (prymnesin-1) was found in the A-type extract (UNCW-ARC140). Two analogs containing two Cl-moieties (prymnesin-A (2 Cl) + pentose and prymnesin-A (2 Cl) + 2 pentose + hexose) were detected in the A-type sample from Sigma Aldrich. The only analog containing two Cl-moieties in the UNCW-ARC140 extract was prymnesin-A (2 Cl + DB) + pentose, which was not found in the solution from Sigma Aldrich. The two B-type samples were more similar to one another, with analog prymnesin-B (1 Cl) accounting for 35 % in the UNCW-ARC66 and 24 % in the K-0881 extract. The dominant analog of the K-0881 extract was prymnesin-B (1 Cl) + hexose (known as prymnesin-B1) with 41 %. The main difference between these two was that no analogs containing 2 Cl were present in the UNCW-ARC66 extract. The most abundant analog in the RCC-1436 extract was prymnesin-C (4 Cl+ DB) + pentose. An estimate of the total concentration (µM) was calculated for each sample based on the analogs present, accounting for all prymnesin analogs. From this point onwards, all concentrations provided will reflect the concentration of the analog mixture of the prymnesin samples.

Table 1Prymnesin profiles of samples used in this project reported as percentages of the total peak areas. The total concentration of the prymnesin sample based on the total analog content is also given (uM)

A-type prymnesins	ARC140	Sigma Aldrich ¹⁾ *
PRM-A (2 Cl + DB) + pentose	12	-
PRM-A (2 Cl) + pentose	-	2
PRM-A (2 Cl) $+$ 2 pentose $+$ hexose	-	4
PRM-A (3 Cl)	6	-
PRM-A (3 Cl) + pentose	43	18
PRM-A (3 Cl) $+$ 2 pentose	4	3
PRM-A (3 Cl) $+$ pentose $+$ hexose	13	9
PRM-A (3 Cl) $+$ pentose $+$ 2 hexose	-	2
PRM-A (3 Cl) $+$ 2 pentose $+$ hexose	21	61
Concentration (µM)	9.1 ± 2.4	2.2 ± 0.2
B-type prymnesins	ARC66	K-0081 ¹
PRM-B (1 Cl)	35	24

B-type prymnesins	ARC66	K-0081 17
PRM-B (1 Cl)	35	24
PRM-B (1 Cl) + pentose	32	18
PRM-B (1 Cl) $+$ hexose	25	41
PRM-B (1 Cl) $+$ pentose $+$ hexose	4	2
PRM-B (1 Cl) $+$ 2 hexose	5	10
PRM-B (2 Cl) sum of all varieties	-	5
Concentration (µM)	22 ± 6	204 ± 18
		1)

Concentration (pivi)	22 ± 0	204 ± 10
C-type prymnesins	RCC-1436 1)	
PRM-C (2 Cl + DB) + pentose	4	
PRM-C (3 $Cl + DB$)	8	
PRM-C (3 Cl + DB) + pentose	17	
PRM-C (3 Cl + DB) + pentose + hexose	1	
PRM-C (3 Cl) $+$ pentose	8	
PRM-C (4 $Cl + DB$)	28	
PRM-C (4 Cl $+$ DB) $+$ pentose	36	
Concentration (µM)	15 ± 1	

[&]quot;-" not detected; DB double bond

3.2. Toxicity of prymnesins

3.2.1. Cytotoxicity

The cytotoxic potential for most samples had already been described in the previous study by Varga and Prause et al. (2024). The A-type prymnesin solution (Sigma Aldrich), the most potent sample, showed a cytotoxic EC50 of about 4 nM in RTgill-W1 cells and 6-7 nM in HCEC-1CT cells. The RCC-1436 C-type prymnesin extract was the second most potent, with EC_{50} values of 14 nM for RTgill-W1 cells and approximately 34 nM for the HCEC-1CT cell line. The extract from the B-type producing strain K-0081 exhibited 50 % cytotoxicity at concentrations of 127 nM and 170 nM, respectively. For the purpose of this study, the two UNCW-ARC strain extracts were evaluated for their cytotoxicity as well. The samples were tested for their toxic effects towards RTgill-W1 cells and measured via CTB. A 50 % cytotoxic effect was observed at approximately 5 nM of the UNCW-ARC140 extract (A-type). The highest concentration of the UNCW-ARC66 extract (B-type),113 nM not exceeding the maximum EtOH concentration of 0.5 % (ν/ν), could decrease metabolic activity to about 60 % only (Supplementary information (SI) Fig. 1).

3.2.2. Hemolytic potential

The difference in potency between the three prymnesin groups (A, B, and C) was tested for hemolysis of RBCs obtained from salmon blood. All tested prymnesin samples were potent hemolysins (Fig. 2). Once again, the A-type solution (Sigma Aldrich) was the most potent, with an approximated HC $_{50}$ value of 6 nM. A 50 % hemolysis (HC $_{50}$) of the RBCs could be achieved at 9 nM of the UNCW-ARC140 A-type extract, and the highest possible concentration of 18.2 nM (maintaining EtOH levels at 0.5 % (ν/ν)) lysed about 70 % of all RBCs. The C-type prymnesin sample had an estimated HC $_{50}$ of about 54 nM, and lastly 600 nM of the B-type extract from strain K-0081 were needed to achieve 50 % lysis of RBCs. The C-type prymnesin sample could only reach a maximal hemolysis of about 60 % at the highest possible concentration while maintaining a 0.5 % (ν/ν) EtOH concentration. The UNCW-ARC66 B-type prymnesin extract was not tested for hemolysis, considering its low cytotoxic potential.

3.3. Impact of sterols on toxicity

3.3.1. Combination assays

In order to assess the influence of sterols on the toxicity, combination assays of toxins with sterols were performed. The samples were diluted to their HC50 or EC50 values and combined with cholesterol or epicholesterol prior to starting the hemolysis or cytotoxicity assays. The total EtOH concentration was kept at 0.5 % (ν/ν), and therefore this percentage was also used for the solvent control (either in Tris buffer or culture medium). In general, standard deviations for the hemolysis experiments were at times larger than expected. This can be explained by the fact that new batches of 1.25 %-RBC solution had to be prepared often, as their shelf-life is unpredictably short (max. 7-10 days). Thus, the replicates for the assays with the K-0081 B-type prymnesin extract as well as the UNCW-ARC140 A-type extract for instance were conducted using different batches of RBC solution, as it would have been wasteful to restart the experiment and discard previously obtained results. The variance between the RBC batches remained at \leq 10 % for all tested saponin concentrations, with the exception of saponin at 1,600 ng/mL (SI Fig. 2). This concentration was right around the HC₅₀ of the saponin control where higher variabilities are always observed. Importantly, the number of RBCs was not counted during the preparation of this solution, which may have had an additional effect on data reproducibility. The Ctype prymnesin sample could not be tested for combination with epicholesterol as insufficient sample volume was available.

Neither cholesterol nor epicholesterol showed any hemolytic activity of their own (SI Fig. 3). For all tested prymnesins, a clear decrease of the hemolytic effect could be observed once the sample had been combined

¹⁾ As previously reported in Varga and Prause et al. (2024).

^{*} Duplicate of the sample reported previously.

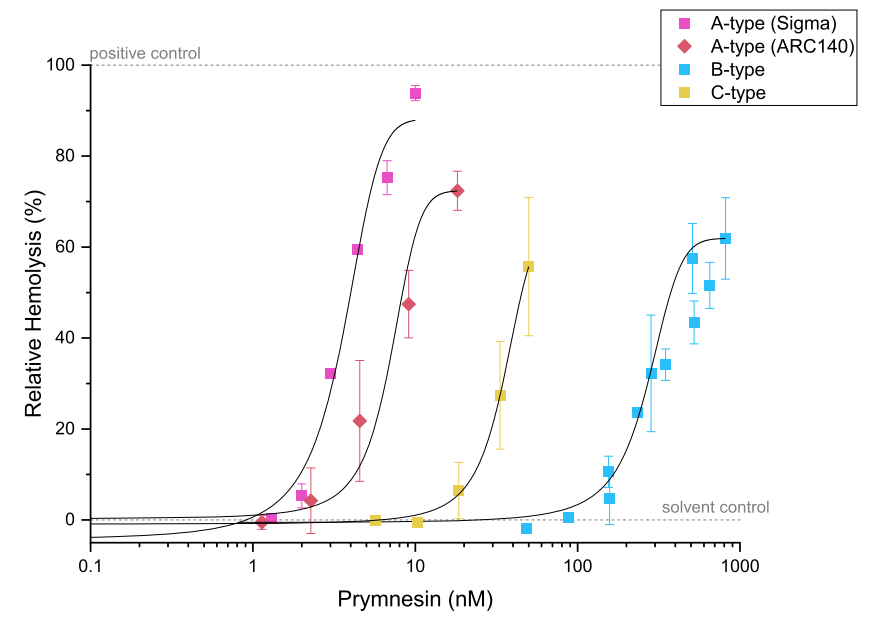


Fig. 2. Hemolytic activity of the A-type solution (Sigma Aldrich), the A-type extract (strain UNCW-ARC140), the B- (strain K-0081), and C-type (strain RCC-1436) prymnesins in red blood cells from Atlantic salmon (Salmo salar). Saponin (8 μ g/mL) was used as positive control and set as 100 % hemolysis, Tris-buffer II containing 0.5 % (ν / ν) EtOH served as solvent control. The prymnesin concentrations (nM) reflect the total concentration of all analogs present in each sample respectively. Data is provided as mean \pm SD of $n \ge 2$.

with sterols (Fig. 3). The reduction of hemolysis was seemingly independent of the sterol concentration, with the addition of sterols at 0.1 nM and 1,000 nM resulting in a similar effect for most samples. Only for the A-type prymnesin solution combination with cholesterol or epicholesterol at 10,000 nM led to an even stronger reduction in hemolysis. This reduction was significantly different from the effect obtained with other concentrations of cholesterol. Remarkably, the combination of A-type prymnesin solution with 10,000 nM cholesterol resulted in practically 0 % hemolysis, while with epicholesterol no smaller value than 10 % hemolysis could be reached. It seems important to note that these effects could not be observed in the combination assays with the A-type prymnesin extract (UNCW-ARC140). In this sample, the observed reduction in hemolysis was stable at all concentrations of added sterols, which was similar to the hemolytic activity observed for the K-0081 B-type prymnesin sample.

Given the outcome of the hemolytic potential after combination with sterols, the question was addressed whether pre-incubation of prymnesins with sterols also affects the cytotoxic potential towards fish gill cells (RTgill-W1) or human epithelial cells (HCEC-1CT) (SI Fig. 4 and SI Fig. 5). Interestingly, no discernible change in cytotoxic potential could be measured when the toxin was pre-incubated with sterol, with the exception of a combination with cholesterol at the lowest concentration of 0.1 nM, where a significant decrease in the cytotoxicity of A-type prymnesins at 4 nM could be calculated for the CTB assay (SI Fig. 4A). In the human cell line HCEC-1CT, the A-type solution (Sigma Aldrich) at 7 nM (EC $_{50}$ adjusted for the cell line) combined with cholesterol at 100 nM, 10,000 nM, and 50,000 nM reduced the cytotoxic potential by about 15 %. Nevertheless, this reduction in cytotoxicity did not show a significant difference and thus remains a trend (SI Fig. 4 A).

3.3.2. Modulation of membrane cholesterol content

The cytotoxic potential of prymnesins was tested on RTgill-W1 cells that had been altered in their cholesterol content. More cholesterol was loaded into the cells by treating them with MbCD-Chol and, for comparison, lovastatin was used to deplete the cells of cholesterol. The resulting change in cholesterol content was determined by staining with filipin and measuring the integrated fluorescent intensity (Fig. 4). A concentration of 10 μM MbCD-Chol was effective in significantly

increasing the cellular cholesterol content by approximately 30 %. Treatment with lovastatin for 24 h also caused a concentration-dependent change in the cholesterol level. Lovastatin lowered the content by about 25 % and 10 % at 10 μM and 1 μM , respectively. None of these treatments impacted the cell viability, as measured in the WST-1 assay (SI Fig. 6).

Once the cholesterol content could be modulated, cholesterol load (MbCD-Chol) and reduction (Lova) were used to explore the dependency of the toxicity of the prymnesins. To evaluate possible changes in cytotoxic potency, the A-type solution (Sigma Aldrich) and the UNCW-ARC66 B-type prymnesin extract at approximately EC90 and EC60, respectively, as well as the A-type extract from strain UNCW-ARC140 at EC₂₀ and EC₇₀ were added to the cells directly after the 24-h cholesterol modulation. Exposure lasted 3 h and the consequent cell damage was measured via the CTB assay (Fig. 5). Despite altering the cholesterol content of the cells no clear change in the cytotoxicity could be measured for either one of the samples. Although a tendency for a lower cytotoxic potential could be observed when the cells had been treated with lovastatin and then exposed to the B-type sample, this effect was not significantly different to the impact on untreated cells. Exposure to the A-type sample (Sigma Aldrich) resulted in a similar outcome. The metabolic activity was decreased to about 5 % in regular as well as in cholesterol-altered RTgill-W1 cells. Also for the UNCW-ARC140 sample, no difference between the untreated cells and cholesterol-modulated cells could be observed for neither of the toxin concentrations applied (EC₂₀, EC₇₀). No difference between cholesterol depleted and enriched cells could be measured for any of the prymnesin samples.

3.4. Surface plasmon resonance (SPR)

To better understand the interaction between prymnesins and sterols, SPR was used to measure binding of A- and B-type prymnesins to cholesterol, epicholesterol, and ergosterol. Because interactions could not be measured for single prymnesin analogs, SPR data are viewed as indications for sterol affinity and not reaction kinetics. The reaction was fitted to a simple 1:1 kinetics model and tested for the accuracy thereof (Chi²). When a mixture of analytes is tested for 1:1 binding, it is assumed that they compete for the immobilized ligand, with binding depending

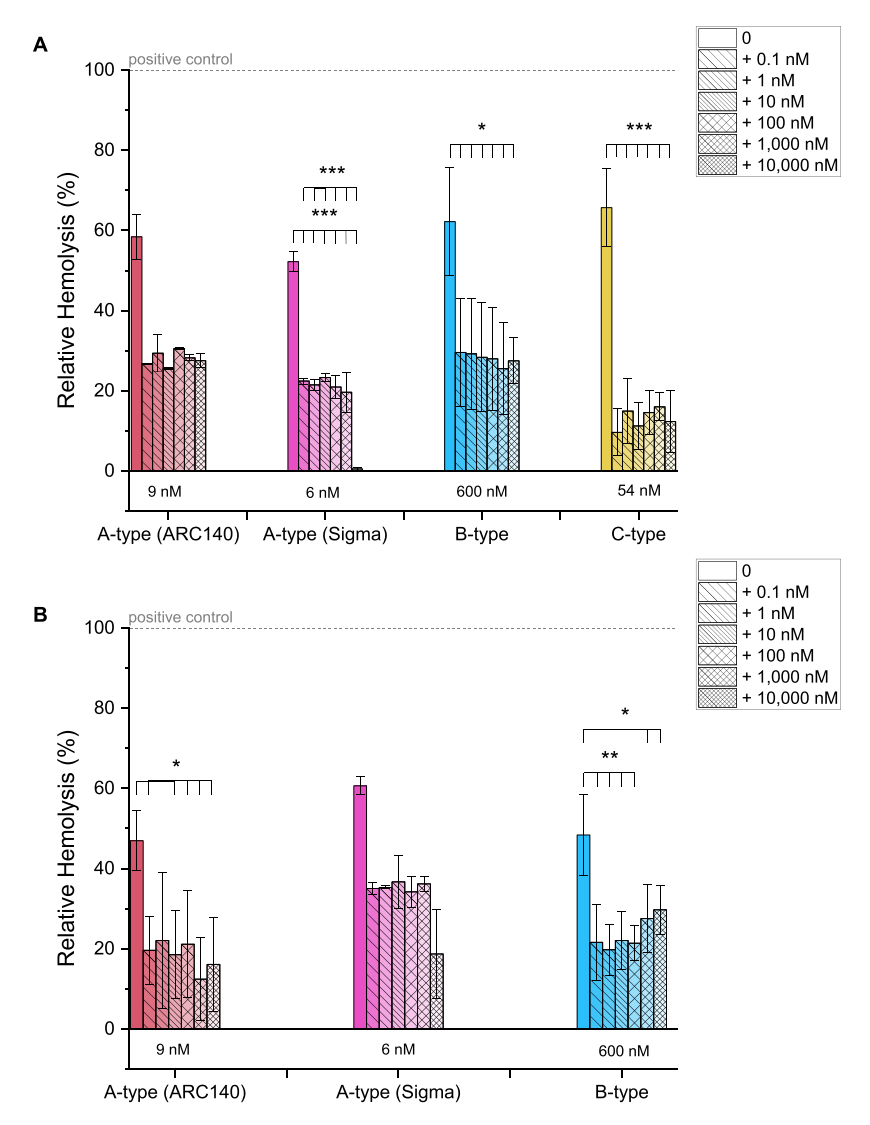


Fig. 3. Potential of both A-type prymnesin samples, the solution from Sigma Aldrich from unknown strain origin and the extract from strain UNCW-ARC140, the extracts from the B-type strain K-0081 and the C-type strain RCC-1436 diluted to their previously established HC_{50} values, compared to hemolytic effects resulting from combination of these samples at their HC_{50} with different concentrations of cholesterol (A) and epicholesterol (B) before incubation with red blood cells. The prymnesin concentrations (nM) reflect the total concentration of all analogs present in each sample respectively. Saponin (8 µg/mL) was used as positive control and set as 100 % hemolysis, and Tris-buffer II containing 0.5 % (ν/ν) EtOH served as solvent control. The sterol control consisted of the highest concentration (10,000 nM) for each sterol in Tris-buffer II and caused 0 % hemolysis. Data is provided as mean \pm SD of n \geq 2. Where the number of replicates equals n = 3 significance was calculated with One Way ANOVA (* = p < 0.05; ** = p < 0.01; *** = p < 0.001). Significance was not calculated for samples with fewer replicates (UNCW-ARC140 sample combined with cholesterol and the Sigma Aldrich solution in combination with epicholesterol).

on analyte concentration and affinity (Gaudreault *et al.*, 2021). Therefore, only the dissociation of the complexes was considered, as dissociation rates are independent of analyte concentrations and can be used to interpret complex stability. The dissociation constants, $k_d(1/2)$, were calculated by the T200 Biacore software and can be found in Table 2. The sensograms are shown in Fig. 6. Both samples, the A-type solution (Sigma Aldrich) and the B-type extract (K-0081) bound to all ligands (sterols), and also non-specifically to the control, octyl-D-glucoside. This unspecific binding can be attributed to the amphipathic properties ascribed to compounds like prymnesins (Andersen *et al.*, 2017; Bachvaroff *et al.*, 2008; Svenssen *et al.*, 2019).

Dissociation rate constants were all within the same range, from 2.59 \times $10^{\text{-}3}$ to 6.72 \times $10^{\text{-}3}$ (1/s), indicating similar complex stability for both toxin mixtures with all three sterols. Notably, no $k_d(1/s)$ was calculated for the A-type sample complexing with cholesterol, as the dissociation range reached RUs below 0. The A-type prymnesin solution seemed to build a more stable complex with epicholesterol, resulting in a $k_d(1/s)$ of

 2.59×10^{-3} , compared to ergosterol (k_d(1/s) of 6.64×10^{-3}). Similarly, the B-type mixture formed the most stable complex with epicholesterol. for which a $k_d(1/s)$ of 3.09×10^{-3} was calculated, followed by the stability of the B-type prymnesins-ergosterol complex. Again, considering that these results stem from a toxin mixture, it should be kept in mind that variances in binding stability may be due to changes in affinities depending on the analogs dominating the interaction. Interestingly though, the fit of the 1:1 model differed between the samples. B-type prymnesins generally fit the 1:1 dissociation much better, with lower Chi² values of 1.97×10^{-1} for ergosterol, 5.45×10^{-1} for cholesterol, and 1.14 for epicholesterol. The A-type sample, in comparison, did not seem to follow a single exponential decay. This suggests that this sample may have a more complex binding interaction with the ligands. Importantly, the RU values for the A-type sample were higher than for the B-type, likely due to the higher EtOH content. This was unavoidable, as the desired concentration of 1 µM required different dilutions of the prymnesin samples.

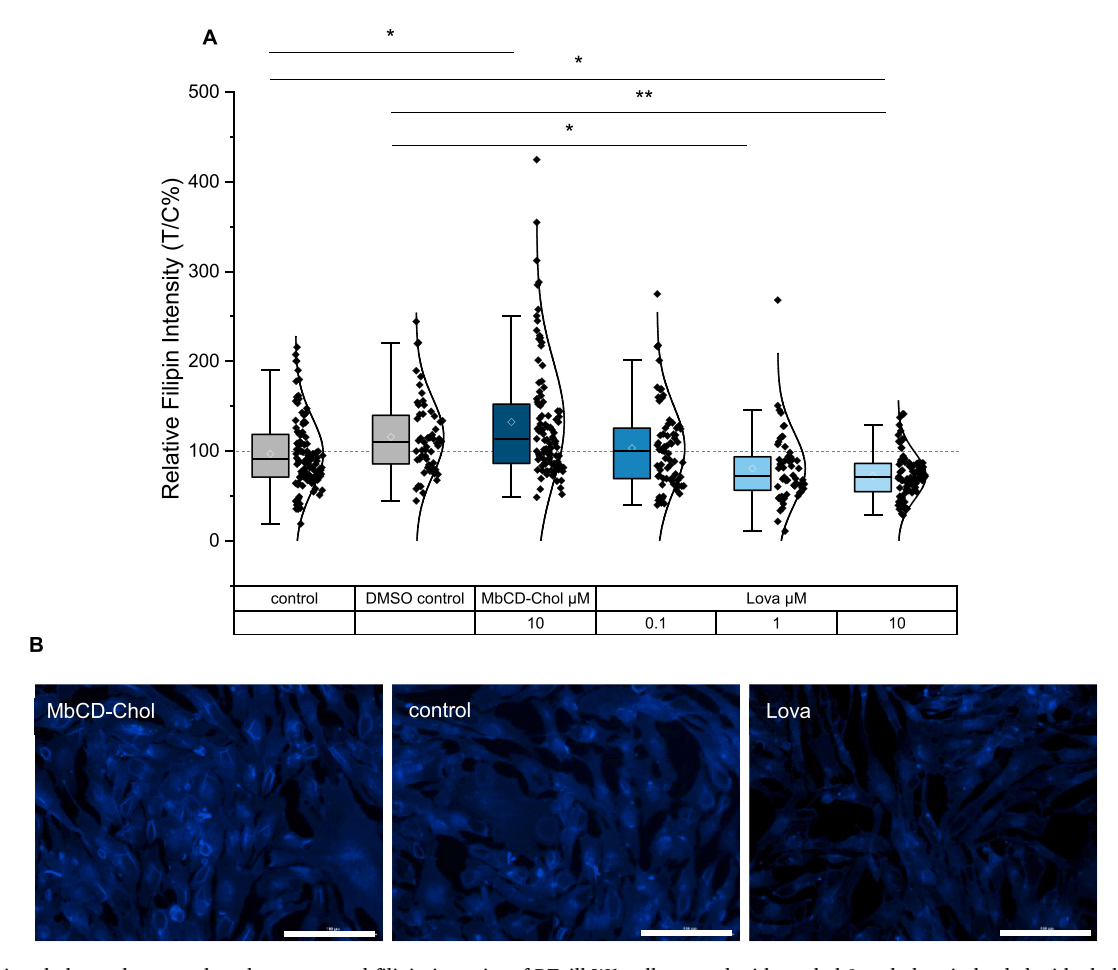


Fig. 4. (A) Relative cholesterol content based on measured filipin intensity of RTgill-W1 cells treated with methyl-β-cyclodextrin loaded with cholesterol (MbCD-Chol) to increase the membrane cholesterol content, and lovastatin (Lova) to deplete the cells of cholesterol. Dimethylsulfoxide (DMSO) at 0.25 % (ν/ν) in culture medium was added as control for treatment with Lova. Unaltered RTgill-W1 cells exposed to culture medium served as control. Data represent mean \pm SD of n=105 cells (7 cells per image, 1 image per well, 3 wells per condition (technical triplicates), 5 biological replicates for each condition (* = p < 0.05; ** = p < 0.01)). (B) RTgill-W1 cells after cholesterol content-modulating treatment stained with filipin. Scale bars represent 100 μm. Lower and upper box boundaries 25th and 75th percentiles, respectively, line inside box median, diamond-shape inside box mean. The black filled diamond shapes represent single data points.

4. Discussion

The observed difference in potency between the two A-type samples used in this study most likely lies in the variability of their analogprofiles. Varga and Prause et al. (2024) have already suggested specific prymnesin analogs to be more cytotoxic than others. It seems the analog prymnesin-A (3 Cl) + 2 pentose + hexose (prymnesin-1) played a key role in A-type sample potency. At the respective EC50, approximately 3.7 nM and 1.9 nM of this analog were present in the A-type solution (Sigma Aldrich) and the UNCW-ARC140 extract, respectively. This would explain the stronger effects observed for the A-type solution (Sigma Aldrich). Prymnesin-A (3 Cl) + pentose (known as prymnesin-2) on the other hand may not be as involved in the toxic mechanism, despite being the most abundant analog in the UNCW-ARC140 extract. Analogs prymnesin-B (1 Cl) + hexose (prymnesin-B1) and prymnesin-B (1 Cl) + pentose (prymnesin-B2) were likely the drivers behind the toxic activity of the B-type samples, as their content in both samples was comparable, and the observed potency was similar as well.

It was shown that the order of cytotoxic potency of A>B>C was also reflected in the hemolytic potential (with approximately 6 nM and 9 nM HC₅₀ for the A-type samples, about 54 nM for the C-type and 600 nM for the B-type sample) (Binzer *et al.*, 2019; Svenssen *et al.*, 2019; Varga and Prause *et al.*, 2024). Intriguingly, the HC₅₀ of 6 nM obtained for the A-type solution (Sigma Aldrich) was very close to the cytotoxic EC₅₀ of 4 nM (1.5-fold increase). The C-type extract was about 10-fold less potent

while the B-type prymnesin extract (strain K-0081) needed a 3.5- to 5-fold EC₅₀ value for hemolysis compared to cytotoxicity. The A-type prymnesin extract (UNCW-ARC140) only needed to be 2-fold more concentrated to reach 50 % hemolysis, which was comparable to the A-type solution (Sigma Aldrich). The procedural variance between the hemolysis and cytotoxicity assays could have impacted the way in which prymnesins target the cells. Although it would be expected that RBCs in suspension are more susceptible than an adherent cell line. Combining prymnesins with sterols before starting hemolysis assays resulted in a significant reduction of hemolytic potential for all tested samples, albeit irrespective of the sterol concentration. This indicates that prymnesins must have interacted with sterols. Previous studies have shown that cholesterol undergoes self-association, forming micelles at a critical concentration of 25 nM to 40 nM at 25 °C. This reversible micelle formation may explain why an increase in cholesterol concentration did not result in an additional decrease in hemolysis (Haberland and Reynolds, 1973). When the micelles are formed it is likely that two phases are created: the aqueous phase containing RBCs, the other the micellar phase into which prymnesins partition due to their lipophilic moiety. Since previous studies on the relevance of cholesterol were conducted using only A-type prymnesins, it was uncertain how B-type prymnesins would perform in such an assay (Igarashi et al., 1998; Imai and Inoue, 1974; Ulitzur and Shilo, 1966). As no strengthened impact on the hemolytic potential was recorded for the other three prymnesin samples, it remains to be examined whether the additional decrease in hemolysis of

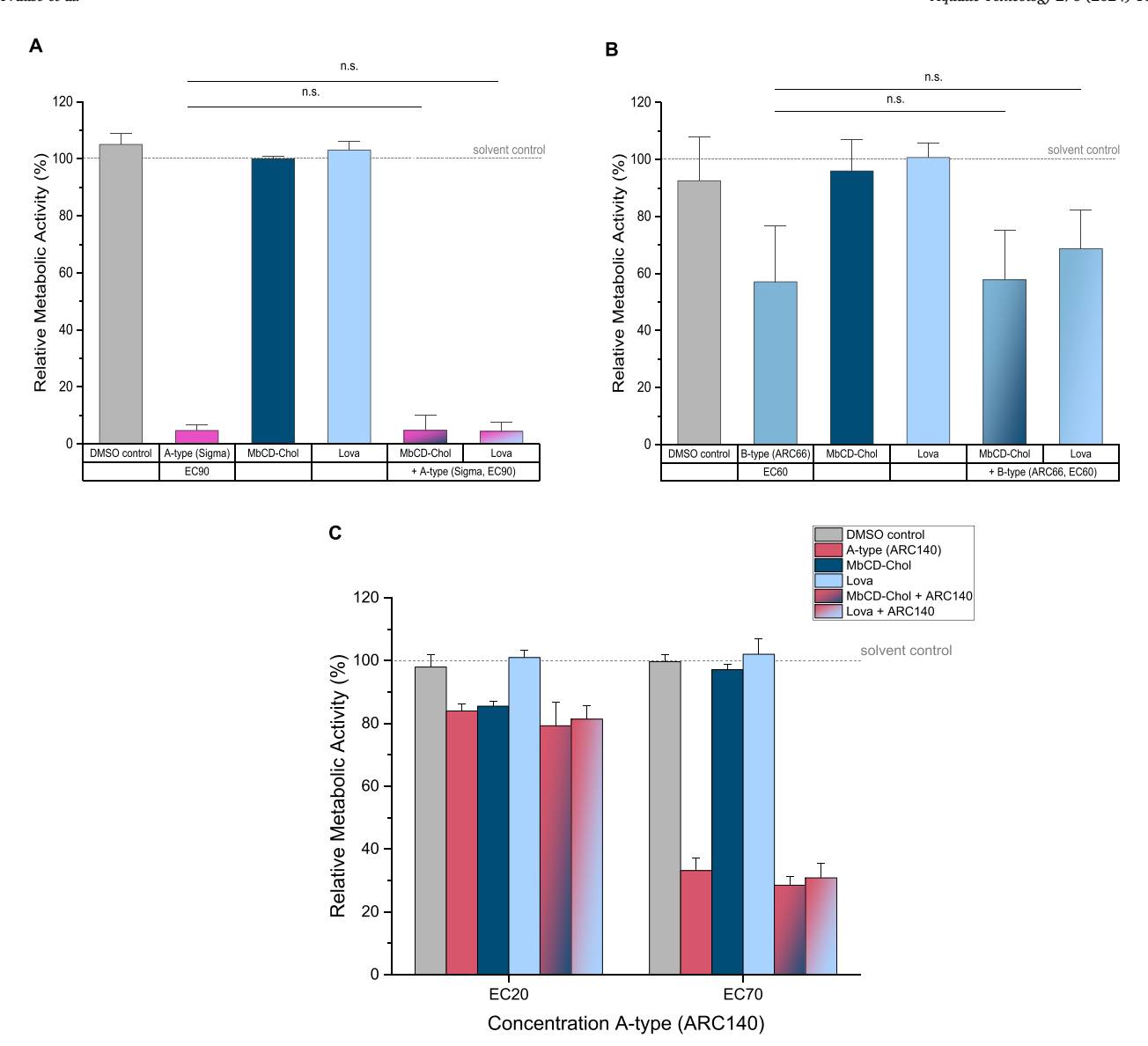


Fig. 5. Metabolic activity of RTgill-W1 cells exposed to the A-type prymnesin solution (Sigma Aldrich) at approximately EC₉₀ (12 nM) (A), the UNCW-ARC66 extract (B-type prymnesins) at approximately EC₆₀ (113 nM) (B), and the UNCW-ARC140 extract (A-type) (C) at approximately EC₂₀ (4 nM) and EC₇₀ (14 nM) for 3 h after a 24 h treatment with the cholesterol-altering compounds methyl-β-cyclodextrin loaded with cholesterol (MbCD-Chol, 10 μM) and lovastatin (Lova, 10 μM). The prymnesin concentrations (nM) reflect the total concentration of all analogs present in each sample respectively. Dimethylsulfoxide (DMSO) at 0.25 % (ν/ν) in culture medium was added as control for treatment with Lova, and culture medium containing 0.5 % (ν/ν) EtOH was used as solvent control. Data represent mean ± SD of n ≥ 3 . (* = p < 0.05; ** = p < 0.01; *** = p < 0.001; n.s. = no significance), except for the ARC140 sample, where sample size was n = 2 (therefore no statistics were performed for this sample).

 $\label{eq:constants} \begin{array}{l} \textbf{Table 2} \\ \text{Dissociation constants k_d (1/s) of the prymnesin samples A-type solution (Sigma Aldrich) and B-type extract (strain K-0081) for the different ligands: cholesterol, epicholesterol, and ergosterol. Chi^2 values indicate the quality of the 1:1 fitting performed for this calculation. \end{array}$

Immobilized ligand	Sample prymnesin	1:1 dissociation k _d (1/s)	Quality Kinetics Chi ² (RU ²)
Cholesterol	A-type B-type	n.d. 6.72×10^{-3}	n.d. 5.45×10^{-1}
Epicholesterol	A-type B-type	$2.59 \times 10^{-3} \ 3.09 \times 10^{-3}$	2.43×10^2 1.14
Ergosterol	A-type B-type	$6.64 \times 10^{-3} \\ 5.35 \times 10^{-3}$	$\begin{array}{l} 5.25 \times 10^{2} \\ 1.97 \times 10^{\text{-}1} \end{array}$

n.d. - no data

the A-type solution (Sigma Aldrich) was caused by something else. Or conversely, whether the presence of unknown compounds in the other samples hindered this effect. As stated in another study, unidentified molecules present in extracts potentially affect the cytotoxic potency of prymnesins (Varga and Prause et al., 2024). The more pronounced differential in potency between the three prymnesin types in the RBCs raises an interesting and potentially important question. The manner in which prymnesins target cell membranes may vary depending on the type of prymnesin and possibly also the specific analog. This variation may become more evident through testing in various cell models. Generally, RBCs from Atlantic salmon were less sensitive toward prymnesins than RTgill-W1 cells, particularly when exposed to B-type and C-type prymnesins. It has already been described in one of the earlier studies on prymnesins that the species origin of RBCs matters greatly when it comes to the hemolytic potential of the analog prymnesin-A (3 Cl) + pentose (Igarashi et al., 1998). This may be caused

H.-C. Prause et al. Aquatic Toxicology 276 (2024) 107080

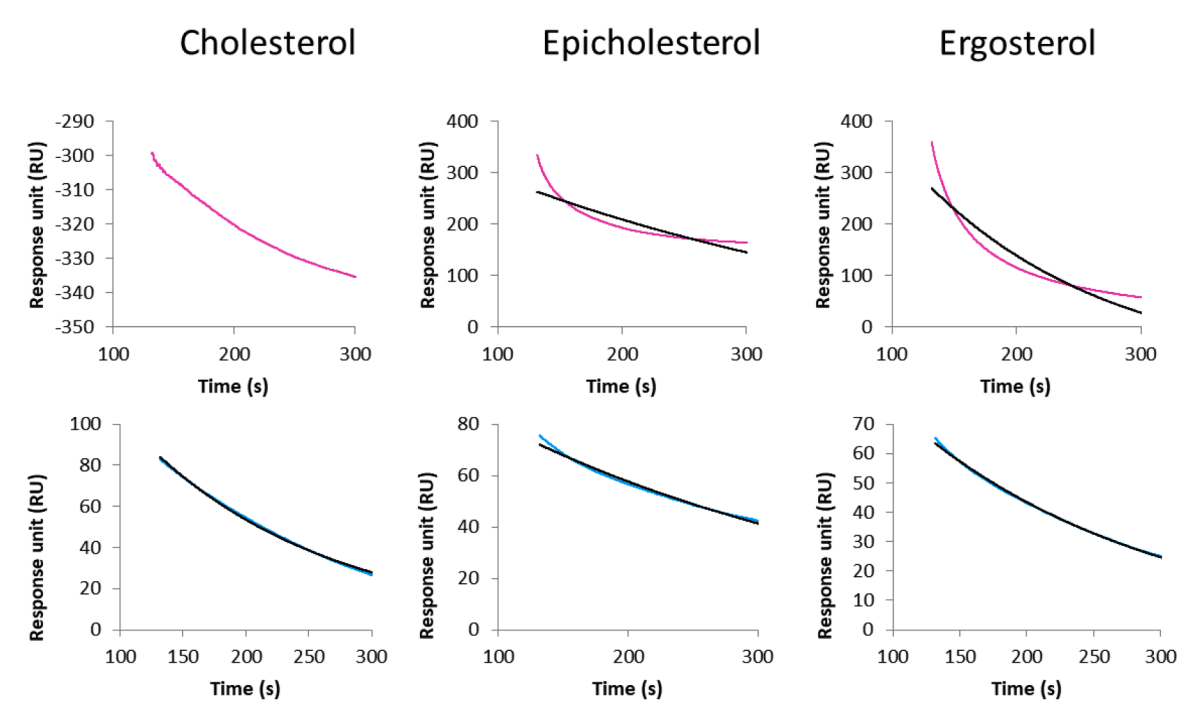


Fig. 6. Sensograms for dissociation kinetics of 1 μ M A-type prymnesins (red (Sigma Aldrich solution from unknown strain origin)) and B-type prymnesins (blue (extract from K-0081)) from immobilized ligands; 10 mM ergosterol, 10 mM epicholesterol, and 10 mM cholesterol. Fitted 1:1 dissociation curves are shown in black and measured curves in color. Measurements were performed in duplicates. The dissociation constants ($k_d(1/s)$) and quality of fit (Chi²) for the respective ligands are provided in Table 2. The prymnesin concentrations (nM) reflect the total concentration of all analogs present in each sample respectively.

by significant variances in lipid profiles in terms of their content of unsaturated and long chain lipids or the cholesterol-phospholipid molar ratio (Cornwell *et al.*, 1968; O'Brien, 1967).

Generally, a change in cholesterol content of about 10-30 % in RTgill-W1 cells could be achieved, yet unexpectedly it did not affect the overall cytotoxicity of the tested samples. Several studies have shown that altering cholesterol content of cells can disrupt the lipid/cholesterol rafts within the plasma membrane (Gyoten et al., 2023; von Tresckow et al., 2004; Zidovetzki and Levitan, 2007). On the one hand, it may be that changes in membrane cholesterol levels did not occur evenly throughout the membrane. One possibility would be that they took place in the cholesterol-rich rafts, leaving cholesterol located outside those rafts available for prymnesin interaction. This theory would at least in part explain why the samples exhibited the same toxicity and seems plausible assuming prymnesins to prefer or be just as capable of interacting with cholesterol outside those lipid rafts. On the other hand, the cholesterol alteration was likely not specifically located in the plasma membrane, but within the entire cell. Previous findings have shown that modifications of plasma cholesterol can have a substantial effect on the intracellular cholesterol content (Lange et al., 2004; Zidovetzki and Levitan, 2007). By this measure, the 10-30 % cholesterol change in the RTgill-W1 cells does not necessarily refer to the plasma membrane only, but to a global cellular cholesterol content. It should be highlighted that while a significant change in cholesterol content could be achieved, continuous lysis induced by prymnesins, possibly to a lower extent, may still be possible even with a lower membrane sterol content.

It was recently suggested that stabilization of pores caused by amphidinol 3 is achieved by insertion of the lipophilic arm through the membrane (Matsumori *et al.*, 2024). Considering that prymnesins and amphidinols share this lipophilic property, it can be inferred that this hydrocarbon chain is of similar importance for prymnesins. They may be able to insert themselves into the bilayer in a way similar to the first binding step of amphidinol 3 or the interaction of saponin with the plasma membrane (Lorent *et al.*, 2014; Matsumori *et al.*, 2024). Seeing how prymnesins are considerably large molecules, self-aggregation of several toxin-entities, as proposed for saponins, seems doubtful (Lorent

et al., 2014). Instead, a prymnesin monomer or dimer may be sufficient to create a channel in the bilayer, enabling ion transport through the membrane as, proposed by the group of Chen et al. (2005) for amphiphilic compounds with a more rigid or more flexible core, respectively. At this point it remains to be debated how flexible prymnesin molecules are, and how much the lack of the double-ring structure in B-types influences this compared to the A-type prymnesins. Considering the SPR data of obtained in this study, it could be suggested that B-type and A-type prymnesins have distinct mechanisms of interacting with the bilayer. A-type prymnesins may exhibit a binding similar to that of amphidinol 3, which follows a two-step binding (Matsumori et al., 2024). The significantly lower potency observed for B- and C-type prymnesins in RBCs may hint at an interaction distinct from that of A-types with the plasma membrane.

Based on the results of this study, it seems as though cellular cholesterol of the target cell is not the defining factor for the mode of action of prymnesins, and that the role of cholesterol must be more intricate. P. parvum cells contain a very low overall level of sterols, which could be considered a self-protection mechanism (Ghosh et al. 1998). This theory would be in line with the fact that prymnesins are able to build stable complexes with cholesterol, as was shown in the SPR experiments. However, modulating the cholesterol content of RTgill-W1 $\,$ cells had no effect on prymnesin cytotoxicity, which contradicts the previous theory. Considering all the findings discussed thus far an alternative hypothesis could be inferred: prymnesins may require cholesterol as an anchor to the cell membrane, yet the actual pore-formation is in part caused or stabilized by a different mechanism. One suggestion is pore-formation through increased activation of selected ion-channels or ATPases (Haberman, 1989; Cox et al. 2019). This hypothesis seems more likely given that prymnesin toxicity is known to be influenced by the presence or absence of certain ions and can affect membrane conductance (Igarashi et al. 1998; Moran and Ilani., 1974; Ulitzur and Shilo, 1964; Varga and Prause et al., 2024). It should be kept in mind, that the exact mechanism might look different between each prymnesin type (A,- B-, or C-type)

In conclusion, the lytic mechanism of prymnesins seems to be more

H.-C. Prause et al. Aquatic Toxicology 276 (2024) 107080

complex than previously believed. The interplay of membrane components with each other and the influence prymnesins may have on this remain to be fully assessed. Thus far, it is evident that prymnesins exhibit strong affinities towards lipids and can induce osmotic imbalance in cells. It is likely that A-type and B-type prymnesins target lipidbilayers differently, possibly due to variations in their backbone structures. Additionally, the extent of their toxic effects varies depending on the cell type, which was particularly evident for B- and C-type prymnesins. However, the potency ranking observed for the samples in this study remained the same across the test-systems, indicating that the relative toxicity of individual analogs was stable. Further studies on the mode of action of prymnesins should prioritize understanding the differences between plasma membranes of various cell types and species. These investigations should not only include lipids, but also proteins such as ion-channels. Lastly, understanding which aspects of the different prymnesin classes are responsible for variations in their toxic potential could help deepen knowledge of the mode of action greatly.

Author declaration

Submission of an article implies that the work described has not been published previously (except in the form of an abstract or as part of a published lecture or academic thesis), that it is not under consideration for publication elsewhere, that its publication is approved by all authors and tacitly or explicitly by the responsible authorities where the work was carried out, and that, if accepted, it will not be published elsewhere in the same form, in English or in any other language, without the written consent of the copyright-holder.

By attaching this Declaration to the submission, the corresponding author certifies that:

- The manuscript represents original and valid work and that neither this manuscript nor one with substantially similar content under the same authorship has been published or is being considered for publication elsewhere.
- Every author has agreed to allow the corresponding author to serve as the primary correspondent with the editorial office, and to review the edited typescript and proof.
- Each author has given final approval of the submitted manuscript and order of authors. Any subsequent change to authorship will be approved by all authors.
- Each author has participated sufficiently in the work to take public responsibility for all the content.

CRediT authorship contribution statement

Hélène-Christine Prause: Writing – review & editing, Writing – original draft, Visualization, Methodology, Investigation, Funding acquisition, Formal analysis, Data curation, Conceptualization. Deniz Berk: Writing – review & editing, Visualization, Investigation, Formal analysis, Data curation. Catharina Alves-de-Souza: Writing – review & editing, Resources. Per J. Hansen: Writing – review & editing, Resources. Thomas O. Larsen: Writing – review & editing, Resources. Doris Marko: Writing – review & editing, Supervision, Resources, Funding acquisition. Giorgia Del Favero: Writing – review & editing, Supervision, Resources, Methodology, Conceptualization. Allen Place: Writing – review & editing, Supervision, Resources, Project administration, Methodology, Funding acquisition, Conceptualization.

Declaration of competing interest

The authors declare that they have no known competing financial interests or personal relationships that could have appeared to influence the work reported in this paper.

Data availability

Data will be made available on request.

Funding

This project was partially funded by the travel grant of the Doctoral School in Chemistry (DoSChem) of the University of Vienna. Furthermore, the research was supported by the University of Vienna, Faculty of Chemistry, Department of Food Chemistry and Toxicology. This research was funded in part by the Austrian Science Fund (FWF) [grant DOI:10.55776/I5707]. C.A.d.S. was funded by COPAS Coastal ANID FB210021. For open access purposes, the author has applied a CC BY public copyright license to any author accepted manuscript version arising from this submission. Open access funding was provided by the University of Veterinary Medicine Vienna.

Acknowledgements

We are grateful for the generous input with the imaging workflows of the Core Facility Multimodal Imaging, member of the VLSI (Vienna Life Science Instruments), Faculty of Chemistry, University of Vienna. Much appreciation is felt for John Stubbelfield, Zohar Laboratory, University of Maryland Baltimore County, for procuring the salmon blood samples. Michael Murphy, Biacore, Cytiva (Danaher Corp., Washington DC, USA), kindly supported the data evaluation for SPR experiments. Tom Shier from the Department of Medicinal Chemistry, College of Pharmacy, University of Minnesota gratefully provided the A-type prymnesin solution previously available from Sigma Aldrich. The pellets of strains UNCW-ARC140 and UNCW-ARC66 were kindly provided by the Algal Resources Collection at the University of North Carolina Wilmington. The RTgill-W1 cell line was provided by Kristin Schirmer, Department of Environmental Toxicology, EAWAG, and the HCEC-1CT cell line by Jerry W. Shay from the UT Southwestern Medical Center. This work is supported by the USDA National Institute of Food and Agriculture through the Food Research Initiative SAS program (award #2021-68012-35922). Peter Frühauf and the Department of Analytical Chemistry at the University of Vienna is acknowledged for the provision of the fluorescence detector and Franz Berthiller of the BOKU University for the opportunity to perform LC-HRMS measurements on the 6550 iFunnel Q-TOF LC-MS system. The authors are grateful to the Mass Spectrometry Centre (MSC), member of the VLSI, Faculty of Chemistry, University of Vienna for technical assistance.

Supplementary materials

Supplementary material associated with this article can be found, in the online version, at doi:10.1016/j.aquatox.2024.107080.

References

Andersen, A., de Medeiros, L., Binzer, S., Rasmussen, S., Hansen, P., Nielsen, K., Jørgensen, K., Larsen, T., 2017. HPLC-HRMS quantification of the ichthyotoxin karmitoxin from Karlodinium armiger. Mar. Drugs 15, 278. https://doi.org/10.3390/ md15090278.

Bachvaroff, T.R., Adolf, J.E., Squier, A.H., Harvey, H.R., Place, A.R., 2008.

Characterization and quantification of karlotoxins by liquid chromatography–mass spectrometry. Harmful. Algae. 7, 473–484. https://doi.org/10.1016/j. hal.2007.10.003.

Bergsson, H., Reducha Andersen, N., Søndergaard Svendsen, M.B., Juel Hansen, P., Fleng Steffensen, J., 2019. Respiratory physiology of European plaice (*Pleuronectes platessa*) exposed to *Prymnesium parvum*. Fishes 4 (2), 32. https://doi.org/10.3390/fishes4020032.

Binzer, S.B., Svenssen, D.K., Daugbjerg, N., Alves-de-Souza, C., Pinto, E., Hansen, P.J., Larsen, T.O., Varga, E., 2019. A., B- and C-type prymnesins are clade specific compounds and chemotaxonomic markers in *Prymnesium parvum*. Harmful. Algae. 81. 10–17. https://doi.org/10.1016/j.hal.2018.11.010.

Blossom, H.E., Rasmussen, S.A., Andersen, N.G., Larsen, T.O., Nielsen, K.F., Hansen, P.J., 2014. *Prymnesium parvum* revisited: relationship between allelopathy,

- ichthyotoxicity, and chemical profiles in 5 strains. Aquat. Toxicol. 157, 159–166. https://doi.org/10.1016/J.AQUATOX.2014.10.006.
- Bols, N.C., Barlian, A., Chirino-Trejo, M., Caldwell, S.J., Goegan, P., Lee, L.E.J., 1994. Development of a cell line from primary cultures of rainbow trout, Oncorhynchus mykiss (Walbaum), gills. J. Fish Dis. 17 (6), 601–611. https://doi.org/10.1111/ j.1365-2761.1994.tb00258.x.
- Chen, W.H., Shao, X.B., Regen, S.L., 2005. Poly (choloyl)-based amphiphiles as pore-forming agents: transport-active monomers by design. J Am Chem S 127 (36), 12727–12735. https://doi.org/10.1021/ja053527q.
- Cichewicz, R.H., Hambright, K.D., 2010. A revised amino group pKa for prymnesins does not provide decisive evidence for a pH-dependent mechanism of *Prymnesium* parvum's toxicity. Toxicon 55 (5), 1035–1037. https://doi.org/10.1016/j. toxicon 2010.02.002
- Cornwell, D.G., Heikkila, R.E., Bar, R.S., Biagi, G.L., 1968. Red blood cell lipids and the plasma membrane. J. Am. Oil. Chem. S 45 (5), 297–304. https://doi.org/10.1007/BF02667099
- Caron, D.A., Lie, A.A., Buckowski, T., Turner, J., Frabotta, K., 2023. The effect of pH and salinity on the toxicity and growth of the golden alga, *Prymnesium parvum*. Protist 174 (1), 125927. https://doi.org/10.1016/j.protis.2022.125927.
- Cox, C.D., Gottlieb, P.A., 2019. Amphipathic molecules modulate PIEZO1 activity. Biochem. Soc. Transact. 47 (6), 1833–1842. https://doi.org/10.1042/BST20190372.
- Dayeh, V.R., Schirmer, K., Lee, L.E., Bols, N.C., 2005. Rainbow trout gill cell line microplate cytotoxicity test. Small-scale Freshwater Toxicity Investigations: Toxicity Test Methods, pp. 473–503. https://doi.org/10.1007/1-4020-3120-3_16.
- Deeds, J.R., Terlizzi, D.E., Adolf, J.E., Stoecker, D.K., Place, A.R., 2002. Toxic activity from cultures of *Karlodinium micrum* (= *Gyrodinium galatheanum*)(Dinophyceae)—a dinoflagellate associated with fish mortalities in an estuarine aquaculture facility. Harmful Algae 1 (2), 169–189. https://doi.org/10.1016/51568-9883(02)00027-6.
- Del Favero, G., Hohenbichler, J., Mayer, R.M., Rychlik, M., Marko, D., 2020. Mycotoxin altertoxin II induces lipid peroxidation connecting mitochondrial stress response to NF-kB inhibition in THP-1 macrophages. Chem. Res. Toxicol. 33 (2), 492–504. https://doi.org/10.1021/acs.chemrestox.9b00378.
- Free, G., Van de Bund, W., Gawlik, B., Van Wijk, L., Wood, M., Guagnini, E., Koutelos, K., Annunziato, A., Grizzetti, B., Vigiak, O., Gnecchi, M., Poikane, S., Christiansen, T., Whalley, C., Antognazza, F., Zerger, B., Hoeve, R.J., Stielstra, H., European Commission. Joint Research Centre, 2023. An EU analysis of the ecological disaster in the Oder River of 2022: lessons learned and research-based recommendations to avoid future ecological damage in EU rivers, a joint analysis from DG ENV, JRC and the EEA. Publications Office of the European Union: Luxembourg. https://doi.org/10.2760/067386.
- Gaudreault, J., Liberelle, B., Durocher, Y., Henry, O., De Crescenzo, G., 2021.

 Determination of the composition of heterogeneous binder solutions by surface plasmon resonance biosensing. Sci. Rep. 11 (1), 3685.
- Ghosh, P., Patterson, G.W., Wikfors, G.H., 1998. Sterols of some marine Prymnesiophyceae. J. Phycol. 34 (3), 511–514. https://doi.org/10.1046/j.1529-8817 1998.340511.x.
- Guillard, R.R.L., 1975. Culture of Phytoplankton for Feeding Marine Invertebrates. Culture of Marine Invertebrate Animals. Springer US, Boston, MA, pp. 29–60. https://doi.org/10.1007/978-1-4615-8714-9 3.
- Gyoten, M., Luo, Y., Fujiwara-Tani, R., Mori, S., Ogata, R., Kishi, S., Kuniyasu, H., 2023. Lovastatin treatment inducing apoptosis in human pancreatic cancer cells by inhibiting cholesterol rafts in plasma membrane and mitochondria. Int. J. Mol. Sci. 24, 16814. https://doi.org/10.3390/ijms242316814.
- Haberland, M.E., Reynolds, J.A., 1973. Self-association of cholesterol in aqueous solution. Proc. Natl. Acad. Sci. 70 (8), 2313–2316. https://doi.org/10.1073/ pngs 70.8.2313
- Habermann, E., 1989. Palytoxin acts through Na⁺, K⁺-ATPase. Toxicon 27 (11), 1171–1187. https://doi.org/10.1016/0041-0101(89)90026-3.
- Hallegraeff, G.M., 1993. A review of harmful algal blooms and their apparent global increase. Phycologia 32, 79–99. https://doi.org/10.2216/10031-8884-32-2-79.1.
- Igarashi, T., Aritake, S., Yasumoto, T., 1998. Biological activities of prymnesin-2 isolated from a red tide alga *Prymnesium parvum*. Nat. Toxins 6, 35–41. https://doi.org/ 10.1002/(SICI)1522-7189(199802)6:1<35::AID-NT7>3.0.CO:2-7.
- Igarashi, T., Satake, M., Yasumoto, T., 1999. Structures and partial stereochemical assignments for prymnesin-1 and prymnesin-2: Potent hemolytic and ichthyotoxic glycosides isolated from the red tide alga *Prymnesium parvum*. J. Am. Chem. Soc. 121, 8499–8511. https://doi.org/10.1021/ja991740e.
- Igarashi, T., Satake, M., Yasumoto, T., 1996. Prymnesin-2: a potent ichthyotoxic and hemolytic glycoside isolated from the red tide alga *Prymnesium parvum*. J. Am. Chem. Soc. 118, 479–480. https://doi.org/10.1021/ja9534112.

- Imai, M., Inoue, K., 1974. The mechanism of action of prymnesium toxin on membranes. Biochim. Biophys. Acta 352, 344–348. https://doi.org/10.1016/0005-2736(74)
- Kaartvedt, S., Johnsen, T.M., Aksnes, D.L., Lie, U., Svendsen, H., 1991. Occurrence of the toxic phytoflagellate *Prymnesium parvum* and associated fish mortality in a norwegian fjord system. Can J Fish Aquat Sci 48, 2316–2323. https://doi.org/ 10.1139/f91.272
- Lange, Y., Ye, J., Steck, T.L., 2004. How cholesterol homeostasis is regulated by plasma membrane cholesterol in excess of phospholipids. Proc. Natl Acad. Sci. 101, 11664–11667. https://doi.org/10.1073/pnas.0404766101.
- Lorent, J.H., Quetin-Leclercq, J., Mingeot-Leclercq, M.P., 2014. The amphiphilic nature of saponins and their effects on artificial and biological membranes and potential consequences for red blood and cancer cells. Org & Biomol Chem 12 (44), 8803–8822. https://doi.org/10.1039/C4OB01652A.
- Matsumori, N., Hieda, M., Morito, M., Wakamiya, Y., Oishi, T., 2024. Truncated derivatives of amphidinol 3 reveal the functional role of polyol chain in sterolrecognition and pore formation. BMCL 98, 129594. https://doi.org/10.1016/j. bmcl.2023.129594.
- Moran, A., Ilani, A., 1974. The effect of prymnesin on the electric conductivity of thin lipid membranes. J. Membr Biol 16, 237–256. https://doi.org/10.1007/
- O'Brien, J.S., 1967. Cell membranes—composition: structure: function. J. Theoretical. Biol. 15 (3), 307–324. https://doi.org/10.1016/0022-5193(67)90140-3.
- Rasmussen, S.A., Meier, S., Andersen, N.G., Blossom, H.E., Duus, J.Ø., Nielsen, K.F., Hansen, P.J., Larsen, T.O., 2016. Chemodiversity of ladder-frame prymnesin polyethers in *Prymnesium parvum*. J. Nat. Prod. 79 (9), 2250–2256. https://doi.org/ 10.1021/acs.inatprod.6b00345.
- Rebhahn, V.I.C., Kiss, E., Marko, D., Del Favero, G, 2022. Foodborne compounds that alter plasma membrane architecture can modify the response of intestinal cells to shear stress *in vitro*. Toxicol. Appl. Pharmacol. 446, 116034 https://doi.org/10.1016/j.taap.2022.116034.
- Shilo, M., 1981. The Toxic Principles of *Prymnesium Parvum*. The Water Environment. Springer US, Boston, MA, pp. 37–47. https://doi.org/10.1007/978-1-4613-3267-1_
- Shilo, M., Aschner, M., 1953. Factors governing the toxicity of cultures containing the phytoflagellate *Prymnesium parvum* Carter. Microbiology 8 (3), 333–343. https://doi. org/10.1099/00221287-8-3-333.
- Svenssen, D.K., Binzer, S.B., Medić, N., Hansen, P.J., Larsen, T.O., Varga, E., 2019. Development of an indirect quantitation method to assess ichthyotoxic B-type prymnesins from *Prymnesium parvum*. Toxins 11, 251. https://doi.org/10.3390/ toxins11050251.
- Ulitzur, S., Shilo, M., 1966. Mode of action of *Prymnesium parvum* ichthyotoxin.
 J. Protozool. 13, 332–336. https://doi.org/10.1111/J.1550-7408.1966.TB01915.X.
- Ulitzur, S., Shilo, M., 1964. A sensitive assay system for determination of the ichthyotoxicity of *Prymnesium parvum*. J. Gen. Microbial. 36, 161–169. https://doi. org/10.1099/00221287-36-2-161.
- Valenti Jr, T.W., James, S.V., Lahousse, M.J., Schug, K.A., Roelke, D.L., Grover, J.P., Brooks, B.W, 2010. A mechanistic explanation for pH-dependent ambient aquatic toxicity of *Prymnesium parvum* Carter. Toxicon 55 (5), 990–998. https://doi.org/ 10.1016/j.toxicon.2009.09.014.
- Varga, E., Prause, H.-C., Riepl, M., Hochmayr, N., Berk, D., Attakpah, E., Kiss, E., Medić, N., Del Favero, G., Larsen, T.O., Hansen, P.J., Marko, D., 2024. Cytotoxicity of *Prymnesium parvum* extracts and prymnesin analogs on epithelial fish gill cells RTgill-W1 and the human colon cell line HCEC-1CT. Arch. Toxicol. 98 (2024), 999–1014. https://doi.org/10.1007/s00204-023-03663-5.
- von Tresckow, B., Kallen, K.-J., von Strandmann, E.P., Borchmann, P., Lange, H., Engert, A., Hansen, H.P., 2004. Depletion of cellular cholesterol and lipid rafts increases shedding of CD30. J. Immunol. 172, 4324–4331. https://doi.org/10.4049/ jimmunol.172.7.4324.
- Waters, A.L., Oh, J., Place, A.R., Hamann, M.T., 2015. Stereochemical studies of the karlotoxin class using NMR Spectroscopy and DP4 chemical-shift analysis: insights into their mechanism of action. Angew. Chem. 127, 15931–15936. https://doi.org/ 10.1002/ange.201507418.
- Yariv, J., Hestrin, S., 1961. Toxicity of the extracellular phase of Prymnesium parvum cultures. J. Gen. Microbiol. 24, 165–175. https://doi.org/10.1099/00221287-24-2-165.
- Zidovetzki, R., Levitan, I., 2007. Use of cyclodextrins to manipulate plasma membrane cholesterol content: Evidence, misconceptions and control strategies. *Biochim et Biophys Act - Biomembranes* 1768, 1311–1324. https://doi.org/10.1016/j. bbamem.2007.03.026.